THE ASTROPHYSICAL JOURNAL, 469:784–793, 1996 October 1

ION VISCOSITY MEDIATED BY TANGLED MAGNETIC FIELDS: AN APPLICATION TO BLACK HOLE ACCRETION DISKS

PRASAD SUBRAMANIAN,[1] PETER A. BECKER,[2] AND MENAS KAFATOS[2]
Center for Earth Observing and Space Research, Institute for Computational Sciences and Informatics, George Mason University, Fairfax, VA 22030-4444
Received 1996 January 8; accepted 1996 April 10

ABSTRACT

We examine the viscosity associated with the shear stress exerted by ions in the presence of a tangled magnetic field. As an application, we consider the effect of this mechanism on the structure of black hole accretion disks. We do not attempt to include a self-consistent description of the magnetic field. Instead, we assume the existence of a tangled field with coherence length $\lambda_{\rm coh}$, which is the average distance between the magnetic "kinks" that scatter the particles. For simplicity, we assume that the field is self-similar, and take $\lambda_{\rm coh}$ to be a fixed fraction ξ of the local disk height H. Ion viscosity in the presence of magnetic fields is generally taken to be the cross-field viscosity, wherein the effective mean free path is the ion Larmor radius $\lambda_{\rm L}$, which is much less than the ion-ion Coulomb mean free path λ_{ii} in hot accretion disks. However, we arrive at a formulation for a "hybrid" viscosity in which the tangled magnetic field acts as an intermediary in the transfer of momentum between different layers in the shear flow. The hybrid viscosity greatly exceeds the standard cross-field viscosity when $(\lambda/\lambda_{\rm L}) \gg (\lambda_{\rm L}/\lambda_{ii})$, where $\lambda = (\lambda_{ii}^{-1} + \lambda_{\rm coh}^{-1})^{-1}$ is the effective mean free path for the ions. This inequality is well satisfied in hot accretion disks, which suggests that the ions may play a much larger role in the momentum transfer process in the presence of magnetic fields than was previously thought. The effect of the hybrid viscosity on the structure of a steady-state, two-temperature, quasi-Keplerian accretion disk is analyzed. The hybrid viscosity is influenced by the degree to which the magnetic field is tangled (represented by $\xi \equiv \lambda_{\rm coh}/H$), and also by the relative accretion rate $\dot{M}/\dot{M}_{\rm E}$, where $\dot{M}_{\rm E} \equiv L_{\rm E}/c^2$ and $L_{\rm E}$ is the Eddington luminosity. We find that ion viscosity in the presence of magnetic fields (hybrid viscosity) can dominate over conventional magnetic viscosity for fields that are tangled on sufficiently small scales.

Subject headings: accretion, accretion disks — black hole physics — magnetic fields — MHD — plasmas

1. INTRODUCTION

1.1. *Background*

Viscosity in accretion disks around compact objects has been the subject of investigation for nearly 20 yr (for a review, see Pringle 1981). It was recognized very early on that ordinary molecular viscosity cannot produce the level of angular momentum transport required to provide accretion rates commensurate with the observed levels of emission in active galaxies, quasars, and galactic black hole candidates (Shakura & Sunyaev 1973). Consequently, the actual nature of the microphysics leading to viscosity in such flows has been the subject of a great deal of speculation. For plane-parallel flows with shear velocity $\boldsymbol{u} = u(y)\hat{z}$, the shear stress is defined as the flux of $\hat{z}$-momentum in the $\hat{y}$-direction. In lieu of a detailed physical model for the process, the work of Shakura & Sunyaev (1973) led to the embodiment of all the unknown microphysics into a single parameter α, defined by writing the shear stress as

$$\alpha P = -\eta \frac{du}{dy}, \tag{1.1a}$$

for plane-parallel flow, or, in an accretion disk,

$$\alpha P = \frac{3}{2} \eta \Omega_{\rm kepl}, \tag{1.1b}$$

where P is the total pressure, η is the dynamic viscosity, and $\Omega_{\rm kepl}$ is the local orbital frequency inside a quasi-Keplerian accretion disk. Note the appearance of the negative sign, which is required so that η is positive-definite. Order-of-magnitude arguments advanced by Shakura & Sunyaev (1973) lead to the general conclusion that $0 < \alpha < 1$. This simulated the development of a large number of theoretical models in which α is treated as a free parameter; in many of these models α is taken to be a constant. This has been partially motivated by the fact that in quasi-Keplerian accretion disks around black holes, observational quantities like the luminosity depend only weakly upon α. This enabled progress to be made without precise knowledge of the microphysical viscosity mechanisms. However, this does not eliminate the need for an understanding of these mechanisms, and without such an understanding, much of the high temporal resolution data being collected by space instrumentation cannot be fully interpreted. Several processes have been suggested to explain the underlying microphysical viscosity mechanism. Initial developments focused on the turbulent viscosity first proposed by Shakura & Sunyaev (1973), and later investigated more rigorously by Goldman & Wandel (1995). Although the presence of turbulence in accretion disks is probably inevitable, it is unclear whether this particular viscosity mechanism will dominate over other processes that may be operating in the same disk, such as radiation viscosity (Loeb & Laor 1992), magnetic viscosity (Eardley & Lightman 1975), and ion viscosity (Paczyński 1978; Kafatos 1988).

The paper is organized as follows. In § 1.2 we provide a general introduction to ion viscosity in accretion disks. In § 1.3 we give a heuristic derivation of ion viscosity in the

[1] psubrama@gmu.edu
[2] Also Department of Physics and Astronomy, George Mason University, Fairfax, VA 22030-4444

absence of magnetic fields. In § 1.4 we discuss the cross-field ion viscosity in the presence of magnetic fields. We also discuss the topology of magnetic fields embedded in accretion disks in § 1.5, and conclude that tangled fields are likely to exist. In § 2 we derive the hybrid viscosity due to ions in the presence of tangled magnetic fields for the general case of a plane-parallel shear flow. We apply our results to quasi-Keplerian two-temperature accretion disks in § 3 and discuss the main conclusions in § 4.

1.2. *Ion Viscosity*

Ion (plasma) viscosity in accretion flows has been previously investigated by Paczyński (1978), Kafatos (1988), Filho (1995), and (Katz 1991). In this process, angular momentum is transferred between different layers in the shear flow by ions that interact with each other via Coulomb collisions. The mean free path for the process is then the Coulomb mean free path. Few detailed astrophysical models have been constructed using the plasma viscosity as the primary means for angular momentum transport because of the presumed sensitivity of this mechanism to the presence of magnetic fields. The effect of the magnetic field is particularly important when the ion gyroradius is less than the Coulomb mean free path *and* the orientation of the local field is perpendicular to the local velocity gradient, because in this case different layers in the shear flow cannot communicate effectively. This point was first raised by Paczyński (1978), who argued that even for very weak fields (as low as 10^{-7} G), this effect is enough to almost completely quench the ion viscosity. This is problematic, since it is very reasonable to expect near-equipartition magnetic fields to be present in an accretion flow, with strengths many orders of magnitude greater than 10^{-7} G.

Implicit in Paczyński's argument is the assumption that the local magnetic field is *exactly perpendicular* to the local velocity gradient. However, near-equipartition magnetic fields would probably be tangled over macroscopic length scales, as evidenced, for example, by simulations of the nonlinear stage of the magnetic shearing instability (Brandenburg et al. 1995; Hawley, Gammie, & Balbus 1995; Matsumoto & Tajima 1995). We argue below that the presence of *tangled* magnetic fields effectively eliminates Paczyński's concern, because ions are able to transfer a significant fraction of their momentum by traveling along field lines connecting two different layers in the shearing plasma. We address the issue of tangled fields being embedded in the accreting plasma further in § 1.5.

1.3. *Field-Free Coulomb Viscosity*

Consider a field-free plasma with Coulomb mean free path λ_{ii} and shear velocity distribution $\boldsymbol{u} = u(y)\hat{z}$, where we set $u(0) = 0$ without loss of generality. The shear stress is equal to the net flux of $\hat{z}$-momentum in the $\hat{y}$-direction. In terms of the field-free dynamic viscosity $\eta_{\rm ff}$ the shear stress is given by

$$-\eta_{\rm ff}\,\frac{du}{dy} \equiv -N_i\sqrt{\frac{kT_i}{2\pi m_i}}\,m_i\,\frac{du}{dy}\,\lambda_{ii}2\,, \tag{1.2}$$

where N_i is the ion number density, m_i is the ion mass, and T_i is the ion temperature (Mihalas & Mihalas 1984). The first factor on the right-hand side of equation (1.2) represents the unidirectional particle flux crossing the $y = 0$ plane, and the second factor is the magnitude of the average $\hat{z}$-momentum carried by particles originating a mean distance λ_{ii} from the plane. The factor of 2 accounts for the transport of particles in both directions across the plane. For pure, fully ionized hydrogen, we have

$$\lambda_{ii} = v_{\rm rms}\,t_{ii} = 1.8 \times 10^5\,\frac{T_i^2}{N_i \ln \Lambda}\,, \tag{1.3}$$

where $\ln \Lambda$ is the Coulomb logarithm, $v_{\rm rms} = (3kT_i/m_i)^{1/2}$ is the root mean square velocity of the Maxwellian distribution, and

$$t_{ii} = 11.4\,\frac{T_i^{3/2}}{M_i \ln \Lambda} \tag{1.4}$$

is the mean time between Coulomb collisions. This yields the standard result for the field-free dynamic viscosity obtained by Spitzer (1962),

$$\eta_{\rm ff} = 2.2 \times 10^{-15}\,\frac{T_i^{5/2}}{\ln \Lambda}\ {\rm g\ cm^{-1}\ s^{-1}}\,. \tag{1.5}$$

Equation (1.5) is valid provided the gas is collisional, which in this case requires that the mean free path of the protons λ_{ii} be much smaller than any macroscopic length scale in the problem. It turns out, however, that for gas accreting onto a black hole, λ_{ii}/R and λ_{ii}/H can exceed unity in general, where R is the local radius and H is the local disk height. In this case, regions that are separated by distances larger than the characteristic length over which the velocity varies $[v/(dv/dR) \sim R]$ can easily exchange particles and therefore momentum as well. In such "nonlocal" situations, the shear stress is no longer simply proportional to the local velocity gradient, and one must solve the full Boltzmann equation in order to study the dynamics of the flow. Another problem that arises involves the shape of the ion velocity distribution. When the ions are not effectively confined to a small region of the flow, the local velocity distribution can become distinctly non-Maxwellian due to the influence of processes occurring far away in the disk. In such circumstances, the very existence of the ion temperature must be called into question.

If this were the whole story, then the construction of disk models using ion viscosity would present formidable challenges. However, so far we have completely neglected the effects of the near-equipartition, tangled magnetic field likely to be present in an actual accretion disk. As we argue below, the presence of such a field will completely alter the conclusions reached above if the coherence length of the field is much less than the local disk height H, because then the ions will be effectively confined to a region of plasma with characteristic size $L \ll H$. If the disk is thin ($H < R$), this also implies $L \ll R$.

1.4. *Cross-Field Coulomb Viscosity*

Next we consider the shear stress exerted by ions inside a plasma containing a magnetic field oriented in the $\hat{z}$-direction and moving with velocity $\boldsymbol{u} = u(y)\hat{z}$, where $u(0) = 0$. Hence the magnetic field is exactly perpendicular to the local velocity gradient. In hot accretion disks, one generally finds that $\lambda_{\rm L} \ll \lambda_{ii}$ for near-equipartition magnetic fields (Paczyński 1978), where

$$\lambda_{\rm L} = 0.95 T_i^{1/2} B^{-1} \tag{1.6}$$

is the Larmor radius of the ions in the presence of a magnetic field B. The shear stress is therefore given by

$$-\eta_{\perp}\frac{du}{dy} \equiv -2N_i\sqrt{\frac{kT_i}{2\pi m_i}}\, m_i \frac{du}{dy}\lambda_{\rm L}\frac{\lambda_{\rm L}}{\lambda_{ii}}\,, \qquad (1.7)$$

where $\eta_{\perp}$ is the cross-field viscosity. This is similar to equation (1.2), except that the magnitude of the average $\hat{z}$-momentum carried by particles crossing the plane is now $\sim(du/dy)\lambda_{\rm L} m_i$ because the particles originate at a mean distance $\sim\lambda_{\rm L}$ from the plane. Another modification is the addition of the factor $(\lambda_{\rm L}/\lambda_{ii})$ which accounts approximately for the efficiency of the momentum transfer process. To understand the efficiency factor, imagine an ion originating on the right side of the plane, and spiraling about a magnetic field line. During one gyration, the particle crosses from the right side of the plane to the left side. Since $\lambda_{\rm L} \ll \lambda_{ii}$ by assumption, the probability that the particle will experience a Coulomb collision with another ion before returning to the right side is $\sim\lambda_{\rm L}/\lambda_{ii}$. Hence this factor gives the mean efficiency of the momentum transfer process. The cross-field viscosity can also be written as

$$\eta_{\perp} = \eta_{\rm ff}\left(\frac{\lambda_{\rm L}}{\lambda_{ii}}\right)^2 = 6.11 \times 10^{-26}\,\frac{N_i^2 \ln\Lambda}{T_i^{1/2}B^2}\,. \qquad (1.8)$$

This expression agrees with the result for this case given by Kaufman (1960), to within a factor of the order of unity. We attribute the discrepancy to the approximate nature of our efficiency factor $(\lambda_{\rm L}/\lambda_{ii})$, which does not take several details like the pitch angle of the spiraling ions into account, and to the fact that we take the ions to be originating exactly at a distance $\lambda_{\rm L}$ away.

Since $(\lambda_{\rm L}/\lambda_{ii})^2 \ll 1$ even for field strengths as low as 10^{-7} G, Paczyński (1978) concluded that the ion viscosity plays a negligible role in determining the disk structure unless the magnetic field essentially vanishes. However, Paczyński's conclusion relies upon the assumption that the magnetic field is exactly perpendicular to the local velocity gradient. We do not believe that this assumption is justified when the magnetic field is created dynamically within the disk, rather than imposed from the outside. When the field is created dynamically in turbulent plasma, it is reasonable to assume that the small-scale field varies randomly in time and space. In such situations, the field is *tangled*, and it is more useful to consider a new, "hybrid" viscosity, where the effective mean free path is limited by the coherence length of the magnetic field. We present a derivation of the hybrid viscosity in § 2, culminating with the expression for $\eta_{\rm hyb}$ in equation (2.14).

1.5. *Tangled Magnetic Fields*

The picture of spatially intermittent magnetic "cells" arising out of a balance between amplification by the Keplerian shear and dissipation due to reconnection was invoked by Eardley & Lightman (1975) in one of the earliest discussions of magnetic viscosity. There have been several revisions of that picture since then, treating the effects of buoyancy and turbulence on the flux tubes. A review of this aspect including a comprehensive reference list can be found in Schramkowski & Torkelsson (1996). Furthermore, recent simulations of the Balbus-Hawley magnetic shearing instability (Brandenburg et al. 1995; Hawley et al. 1995; Matsumoto & Tajima 1995) indicate that the magnetic field will be tangled over macroscopic length scales. This has motivated us to assume the existence of a tangled magnetic field, although we do not self-consistently model the generation of the field. The models we present in this paper assume the field to be tangled in a self-similar manner with respect to disk height. In particular, we take the parameter $\xi \equiv \lambda_{\rm coh}/H$ to be a constant, where $\lambda_{\rm coh}$ is the coherence length of the magnetic field. While this might not be satisfied in a realistic scenario, the expressions we derive for the viscosity do accommodate the possibility of a ξ which varies with radius and are therefore sufficiently general. It might be noted that treatments of the magnetic shearing instability suggest that the most rapidly growing eigenmode of the instability has a spatial size that is a fixed fraction of the local disk height (e.g., Matsumoto & Tajima 1995).

2. ION VISCOSITY IN THE PRESENCE OF A TANGLED MAGNETIC FIELD

In § 1.4, we considered the case of a shearing plasma containing a magnetic field oriented in the $\hat{z}$-direction, exactly perpendicular to the local velocity gradient. In an actual accretion disk, we do not expect this to be the case very often. Instead, the direction of the field is likely to be a random function of position on scales exceeding the correlation length of the tangled magnetic field, which arises from MHD turbulence. It is therefore interesting to consider the shear stress exerted by ions in the general case of a randomly directed field. If $\lambda_{\rm L} \ll \lambda_{ii}$, then we expect that ions moving between different layers in the fluid will spiral tightly around the field lines, in which case two of the components of the ion momentum are obviously not conserved. On the other hand, the component of the ion momentum *parallel* to the magnetic field *is* conserved until the particle either experiences a Coulomb collision with another ion or encounters an irregularity in the magnetic field. Hence the transfer of momentum from one layer to another occurs via the component of the particle momentum parallel to the magnetic field, and in this sense the particles act like beads sliding along a string, in what is commonly referred to as the ideal MHD approximation.

The irregularities that scatter the ions may appear as either stationary "kinks" or fast, short-wavelength electromagnetic waves depending on the details of the turbulence. If the particles interact with the field primarily via wave-particle scattering, then the waves must be explicitly included as a dynamical entity in the momentum transfer process. In fact, the shear stress due to the waves themselves may dominate the situation if the wave energy density surpasses that of the particles. However, such large wave energy densities cannot be created if the field is generated dynamically within the plasma, as we assume here. Furthermore, the relatively fast-moving ions that carry momentum in our picture will not often encounter short-wavelength electromagnetic waves with sufficient amplitude to scatter them very strongly. Conversely, the ions *will* be strongly scattered by encounters with long-wavelength, slow-moving kinks in the magnetic field. We therefore ignore the dynamical consequences of the fast waves, and treat the irregularities as stationary kinks.

If the field is frozen into the plasma, then the ion momentum will ultimately be transferred to the local gas via either Coulomb collisions or encounters with magnetic irregularities. The probability per unit length for either type of interaction to occur is proportional to the reciprocal of the associated mean free path. It follows that if the two types of interactions are statistically uncorrelated, then the *effective mean free path* λ is given by

$$\frac{1}{\lambda} = \frac{1}{\lambda_{ii}} + \frac{1}{\lambda_{\rm coh}} , \tag{2.1}$$

where $\lambda_{\rm coh}$ is the mean distance between kinks in the field, which is equivalent to the coherence or correlation length.

We will continue to focus on the case of a plane-parallel shear flow characterized by the velocity distribution

$$\boldsymbol{u} = u(y)\hat{z} , \tag{2.2}$$

where $u(0) = 0$. To eliminate unnecessary complexity, we will also assume that the ions are isothermal with temperature T_i. This is reasonable so long as the temperature does not vary on scales shorter than the ion effective mean free path λ. It will be convenient to introduce a local polar coordinate system (r, θ, ϕ) using the standard transformation

$$x = r \sin\theta \cos\phi , \quad y = r \sin\theta \sin\phi , \quad z = r \cos\theta , \tag{2.3}$$

in which case the velocity v_r along the $\hat{r}$-direction is related to v_x, v_y, and v_z by

$$v_r = v_x \sin\theta \cos\phi + v_y \sin\theta \sin\phi + v_z \cos\theta . \tag{2.4}$$

Let us first consider a case with no magnetic field. Then, viewed from a frame comoving with the local fluid, the local ions have a Maxwellian velocity distribution with temperature T_i. However, viewed from the rest frame of the fluid located at $y = 0$, the distributions of v_x, v_y, and v_z for particles located at an arbitrary value of y are given by

$$f(v_x) = \left(\frac{m_i}{2\pi k T_i}\right)^{1/2} \exp\left(-\frac{m_i}{2kT_i} v_x^2\right) ,$$

$$f(v_y) = \left(\frac{m_i}{2\pi k T_i}\right)^{1/2} \exp\left(-\frac{m_i}{2kT_i} v_y^2\right) ,$$

$$f(v_z) = \left(\frac{m_i}{2\pi k T_i}\right)^{1/2} \exp\left\{-\frac{m_i}{2kT_i} [v_z - u(y)]^2\right\} , \tag{2.5}$$

due to the presence of the shear flow, where $f(v_i)dv_i$ gives the fraction of particles with ith component of velocity between v_i and $v_i + dv_i$, and $\int_{-\infty}^{\infty} f(v_i)dv_i = 1$. Since v_x, v_y, and v_z are independent random variables, it follows from equation (2.4) that the distribution of v_r is given by

$$f(v_r) = \left(\frac{m_i}{2\pi k T_i}\right)^{1/2} \exp\left\{-\frac{m_i}{2kT_i} [v_r - u(y)\cos\theta]^2\right\} . \tag{2.6}$$

Next we consider the effect of "turning on" a magnetic field oriented in the $\hat{r}$-direction specified by the angles (θ, ϕ). If the field is so strong that $\lambda_{\rm L} \ll \lambda_{ii}$, then the ions spiral tightly around the field lines. However, the component of the velocity parallel to the field (v_r) is completely unaffected, and therefore the distribution of v_r is still given by equation (2.6) even in the presence of a magnetic field.

We wish to compute the $\hat{y}$-directed flux of $\hat{z}$-momentum due to particles crossing the $y = 0$ plane from both sides along the field line. It may be noted that since we assume $u(0) = 0$, layers on either side of this plane will have oppositely directed flow velocities. Since we expect that $\lambda_{\rm L} \ll \lambda_{ii}$ in most cases of interest, we shall adopt the "bead-on-string" model for the particle transport and work in the limit $\lambda_{\rm L}/\lambda_{ii} \to 0$, in which case v_y and v_z are given by

$$v_y = v_r \sin\theta \sin\phi , \quad v_z = v_r \cos\theta . \tag{2.7}$$

Hence we ignore the components of momentum perpendicular to the field and consider only the transport of momentum along the field lines. For the purpose of calculating the momentum flux, it is sufficient to consider particles starting out at a distance λ from the origin. It follows that at the starting point

$$y = \lambda \sin\theta \sin\phi , \tag{2.8}$$

and therefore

$$u(y) = u'(0)\lambda \sin\theta \sin\phi \tag{2.9}$$

to first order in λ, where the prime denotes differentiation with respect to y. The $\hat{y}$-directed flux of $\hat{z}$-momentum due to particles approaching the origin from both sides of the $y = 0$ plane is given by

$$P(\theta, \phi) = 2\int_{-\infty}^{0} (m_i v_z)[N_i v_y f(v_r) dv_r] , \tag{2.10}$$

where the first term inside the integral is the $\hat{z}$-momentum carried by the particles and the second term is the $\hat{y}$-directed particle flux. Then to first order in λ we obtain

$$P(\theta, \phi) = 2m_i N_i \cos\theta \sin\theta \sin\phi \times \left[\frac{kT_i}{2m_i} - \left(\frac{2kT_i}{\pi m_i}\right)^{1/2} u'(0)\lambda \cos\theta \sin\theta \sin\phi\right] , \tag{2.11}$$

which gives the shear stress as a function of θ and ϕ. The first term on the right-hand side describes the "thermal stress" due to the stochastic drifting of particles along the field lines, which occurs even in the absence of a velocity gradient. The second term gives the modification due to the presence of the velocity gradient. Equation (2.11) vanishes when the field is exactly perpendicular to the velocity gradient ($\sin\theta \sin\phi = 0$), which agrees with equation (1.8) for the cross-field viscosity in the limit $\lambda_{\rm L}/\lambda_{ii} \to 0$.

Equation (2.11) for the direction-dependent stress can be used to construct two-dimensional models that treat both the radial and azimuthal structure of the disk. In these models, the direction of the local magnetic field is a random function of the radial and azimuthal position on scales exceeding the coherence (correlation) length $\lambda_{\rm coh}$. In order to construct one-dimensional models, we need to average equation (2.11) over all directions to obtain the mean stress

$$\langle P \rangle \equiv \frac{1}{4\pi} \int P(\theta, \phi) d\Omega , \tag{2.12}$$

where $d\Omega = \sin\theta\, d\theta\, d\phi$, and $0 < \theta < \pi$, $0 < \phi < 2\pi$. Substituting equation (2.11) into equation (2.12) and integrating over θ and ϕ yields for the mean (direction-averaged) hybrid viscosity

$$\eta_{\rm hyb} \equiv -\frac{\langle P \rangle}{u'(0)} = \frac{2}{15} m_i N_i \lambda \left(\frac{2kT_i}{\pi m_i}\right)^{1/2} . \tag{2.13}$$

Note that the "thermal stress" appearing in equation (2.11) is symmetric and therefore it vanishes upon integration.

We can also write the hybrid viscosity given by equation (2.13) as

$$\eta_{\rm hyb} = \frac{2}{15}\frac{\lambda}{\lambda_{ii}}\eta_{\rm ff} , \tag{2.14}$$

where $\eta_{\rm ff}$ is the standard, field-free Coulomb viscosity given by equation (1.5). We see that no factor describing the efficiency of the momentum transfer process appears in the expression for $\eta_{\rm hyb}$, in contrast to the cross-field viscosity $\eta_\perp$ given by equation (1.8). This is because in the hybrid case particles originating on the right side of the plane and crossing over definitely deposit their momentum on the left side, since the two planes in question are linked by a field line along which the particle "slides." Since $\eta_{\rm hyb}/\eta_{\rm ff} \sim (\lambda/\lambda_{ii})$ and $\eta_\perp/\eta_{\rm ff} \sim (\lambda_{\rm L}/\lambda_{ii})^2$, it is clear that the hybrid viscosity will greatly exceed the cross-field viscosity if $(\lambda/\lambda_{\rm L}) \gg (\lambda_{\rm L}/\lambda_{ii})$, which is likely to be well satisfied in hot accretion disks, as will be seen in § 3. This suggests that the ions play a much larger role in the momentum transfer process in the presence of magnetic fields than originally concluded by Paczyński (1978). In § 3 we use our results to analyze the structure of a two-temperature quasi-Keplerian accretion disk with unsaturated inverse-Compton cooling.

3. APPLICATION TO TWO-TEMPERATURE ACCRETION DISKS

We consider the two-temperature, steady-state model first proposed by Shapiro, Lightman, & Eardley (1976) and adopted by Eilek & Kafatos (1983). The model assumes that the disk is quasi-Keplerian; i.e., the azimuthal velocity v_ϕ is equal to the Keplerian value and the radial velocity $v_r \ll v_\phi$. In this model the ions and electrons are coupled only via Coulomb collisions and the electrons with temperature T_e are assumed to radiate their energy away via unsaturated inverse-Compton cooling. In this case the two-temperature condition $T_i \gg T_e$ is satisfied if

$$t_{ei} > t_{\rm accr} , \tag{3.1}$$

while in order for the ions and electrons to achieve their respective Maxwellian distributions, we must have

$$t_{\rm accr} > t_{ii} > t_{ee} , \tag{3.2}$$

where t_{ei}, t_{ee}, and t_{ii} are the time scales for electron-ion, electron-electron, and ion-ion Coulomb equilibration, respectively, and $t_{\rm accr}$ is the time scale for accretion onto the black hole. We will use the viscosity prescription given by equation (2.13), and we will assume that the coupling between ions and electrons occurs exclusively via Coulomb interactions. Hence we neglect the possibility that collective plasma processes might result in an additional coupling between the ions and electrons, over and above the usual Coulomb coupling, which could in principle lead to a violation of the two-temperature condition. However, Begelman & Chiueh (1988) considered this possibility, and concluded that such collective processes are not likely to strongly affect the thermal structure of the disk. Equations (A1)–(A6) in Appendix A list the basic structure equations for the two-temperature quasi-Keplerian disk model. Equations (A7)–(A9) in Appendix A constitute a list of the analytical solutions to these structure equations, which are derived under the assumption that $T_i \gg T_e$. These solutions have an arbitrary α parameter built into them, which in general can be treated as a constant or allowed to vary with radius using a specific model for the viscosity. In our case the variation of α is obtained by substituting our expression for $\eta_{\rm hyb}$ into equation (1.1).

In order to close the system of equations and obtain solutions for the disk structure, we must also adopt a model for the variation of the magnetic coherence length $\lambda_{\rm coh}$ which appears in the definition of the effective mean free path λ (eq. [2.1]). We assume here that the field topology varies in a self-similar manner with the local height H, so that

$$\lambda_{\rm coh} \equiv \xi H , \tag{3.3}$$

where ξ is a free parameter which we set equal to a constant for a given model.

3.1. *A Two-Temperature Accretion Disk Model*

In a cylindrically symmetric accretion disk, the relevant component of the stress arising from the hybrid viscosity is given by

$$\alpha_{\rm hyb} P \equiv -\eta_{\rm hyb} R \frac{d\Omega_{\rm kepl}}{dR} , \tag{3.4}$$

which is equivalent to equation (1.1). We use equation (3.4) to derive $\alpha_{\rm hyb}$ from $\eta_{\rm hyb}$. Equations (A7)–(A9) in Appendix A and equation (3.4) jointly yield the following self-consistent solutions for the model:

$$\alpha_{\rm hyb} = 147.31\,\delta^{1/3} f_1^{-1/6} f_2^{2/3}\left(\frac{\dot M_*}{M_8}\right)^{2/3} \tau_{\rm es}^{-1} R_*^{-1} , \tag{3.5}$$

$$T_i = 3.38 \times 10^{11}\,\delta^{-1/3} f_1^{1/6} f_2^{1/3}\left(\frac{\dot M_*}{M_8}\right)^{1/3} R_*^{-1/2} , \tag{3.6}$$

$$T_e = \frac{1.40 \times 10^9 y}{\tau_{\rm es}(1+\tau_{\rm es})} , \tag{3.7}$$

$$N_i = 5.70 \times 10^{11}\,\delta^{1/6} f_1^{5/12} f_2^{-1/6}\left(\frac{\dot M_*}{M_8}\right)^{5/6} \dot M_*^{-1} \tau_{\rm es} R_*^{-5/4} \tag{3.8}$$

$$\frac{H}{R} = 0.175\,\delta^{-1/6} f_1^{-5/12} f_2^{1/6}\left(\frac{\dot M_*}{M_8}\right)^{1/6} R_*^{1/4} , \tag{3.9}$$

where

$$\delta \equiv \frac{\lambda}{\lambda_{ii}} = \left(1 + \frac{\lambda_{ii}}{\xi H}\right)^{-1} , \tag{3.10}$$

and

$$\dot M_* \equiv \frac{\dot M}{1\ M_\odot\ {\rm yr}^{-1}} , \quad M_8 \equiv \frac{M}{10^8\ M_\odot} , \quad R_* \equiv \frac{R}{GM/c^2} . \tag{3.11}$$

The following two equations jointly define an implicit algebraic equation for determining δ as a function of R_* for given $(\xi, y, \dot M_*/M_8)$

$$\tau_{\rm es} = 915.508\xi^{-1}\frac{\delta^{1/3}}{1-\delta} f_1^{1/3} f_2^{2/3}\left(\frac{\dot M_*}{M_8}\right)^{2/3} R_*^{-1} \tag{3.12}$$

$$\tau_{\rm es}^{7/3}(1+\tau_{\rm es}) = 57.8819\,\delta^{1/9} f_1^{-7/18} f_2^{-1/9} f_3^{2/3} y\left(\frac{\dot M_*}{M_8}\right)^{5/9} R_*^{-5/6} . \tag{3.13}$$

We will restrict our attention to $1 > \xi > 0$, since $\xi \gtrsim 1$ implies that the field is strongly ordered over macroscopic length scales, which violates our assumption that the field is tangled. Once a root for δ is determined for a given ξ, it is used in equation (3.12), and the result obtained for τ_{es} is then used in equations (3.5)–(3.9) to determine the disk structure. For instance, δ ranges between 10^{-6} and 10^{-7} for the model shown in this paper. The small value of δ is indicative of the fact that the mean free path is determined primarily by λ_{coh} and not by λ_{ii}. In principle, one could compute a disk model for a given y and any combination of ξ, $\dot{M}_*$, and M_8. We consider $0.001 < \dot{M}/\dot{M}_E < 1$, where $\dot{M}_E = L_E/c^2$ and $L_E = 4\pi G M m_p c/\sigma_T$ is the Eddington luminosity and σ_T is the Thomson cross section. Note that $\dot{M}_E = 0.22\ \dot{M}_*/M_8$. Accretion rates that are close to the Eddington value are more likely to be significant from the point of view of observations.

3.2. *Model Self-Consistency Constraints*

For the models to be self-consistent, they have to fulfill the following conditions.

(i) $H/R < 1$. This ensures that the disk remains geometrically thin and is assumed in deriving the analytical solutions listed in Appendix A.

(ii) $\lambda/H < 1$. This condition ensures that the magnetic field lines are confined within the disk. Since $\xi \equiv \lambda/H$ is a free parameter in our model and we restrict our attention to $\xi < 1$, this condition is automatically satisfied.

(iii) $\lambda/R < 1$. This assures us of the validity of applying the fluid approximation to the plasma. Imposing $\xi \equiv \lambda/H < 1$ and ensuring $H/R < 1$ results in the satisfaction of this criterion.

(iv) $T_i/T_e > 1$. Satisfaction of the two-temperature condition is assumed in deriving the analytical solutions in Appendix A.

3.3. *Comparison with Other Kinds of Viscosity*

Of the different kinds of viscosity that can possibly exist in the accretion disk, we assume the hybrid viscosity we have derived here to be the dominant form. We would like to compute other possible forms of viscosity a posteriori, and compare them with the hybrid viscosity. The hydrodynamic turbulent viscosity used by Shakura & Sunyaev (1973) is based on dimensional arguments, and, according to Schramkowski & Torkelsson (1995), is probably less significant than viscosity arising from MHD turbulence, in which the magnetic field plays a significant role. For relatively high accretion rates, one would expect rather high luminosities. Consequently, the contribution of radiation viscosity, which is characterized by an associated α_{rad}, would be appreciable. Magnetic viscosity (characterized by α_{mag}), which arises from the stresses associated with the tangled magnetic field, is another important form of viscosity with which we compare the hybrid viscosity obtained from our calculations. Appendix B describes how α_{rad} is calculated. We describe how α_{mag} is calculated below. In particular, it may be noted that we need to adopt a different definition of the coherence length λ_{coh}, given by equation (3.15), in order to quantify α_{mag}.

If we consider the magnetic stress to be equal to the magnetic pressure $P_B = B^2/(8\pi)$, the α parameter arising out of pure magnetic viscosity is defined by

$$\alpha_{mag} P \equiv \frac{B^2}{8\pi}, \tag{3.14}$$

where P is the total pressure. It is customary to use the following definition for λ_{coh} in discussions of magnetic viscosity,

$$\lambda_{coh} = \frac{V_A}{\Omega_{kepl}}, \tag{3.15}$$

where V_A is the Alfvén speed. This formula arises from a balance between amplification of the field by shear and dissipation due to reconnection. Vertical hydrostatic equilibrium can be expressed as

$$P = \tfrac{1}{6}\Omega_{kepl}^2 \rho H^2 . \tag{3.16}$$

Combining equations (3.14), (3.15), and (3.16) gives

$$\alpha_{mag} = \left(\frac{\lambda_{coh}}{H}\right)^2 . \tag{3.17}$$

In our models, $\xi \equiv \lambda_{coh}/H$ is a free parameter, and equation (3.17) reduces to $\alpha_{mag} = \xi^2$.

3.4. *Results*

Figure 1 shows a parameter space plot for a canonically rotating Kerr black hole ($a/M = 0.998$). Each point in the parameter space spanned by ξ and $\dot{M}/\dot{M}_E$ represents a potential model. Each of these models assumes a constant

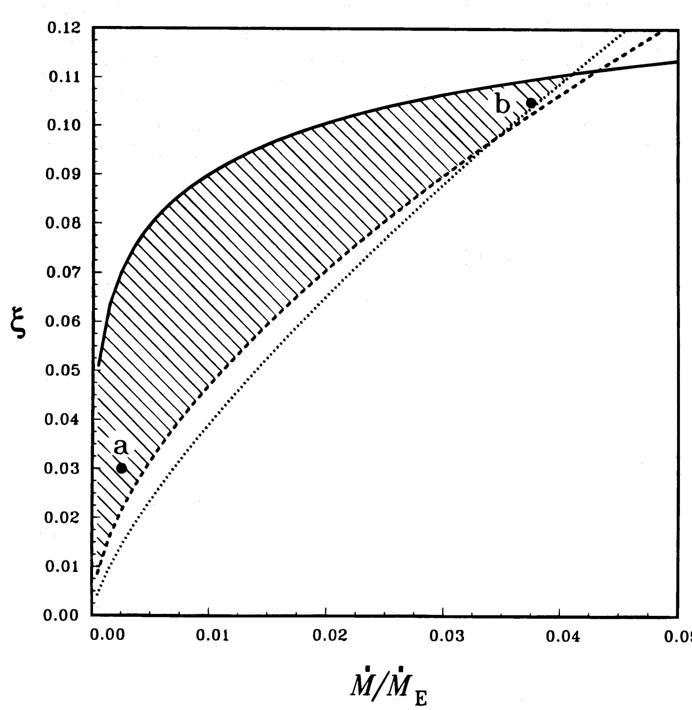

FIG. 1.—The (ξ, $\dot{M}/\dot{M}_E$) parameter space for the canonical Kerr metric with $a/M = 0.998$. Each point in the parameter space represents a potential model. The disk is assumed to occupy the range $R_{ms} < R_* < 50$, where R_{ms} is the radius of marginal stability in gravitational radii. For this range of radii, models with parameters lying below the solid line fulfill $\alpha_{hyb} > \alpha_{mag}$; those with parameters lying above the dotted line fulfill $H/R < 1$; those with parameters lying above the dashed line fulfill $\alpha_{hyb} > \alpha_{rad}$. The condition $T_i > T_e$ is fulfilled throughout the parameter space shown. The shaded region is the one in which our models are self-consistent insofar as conditions (i)–(iv) described in § 3.2 are concerned.

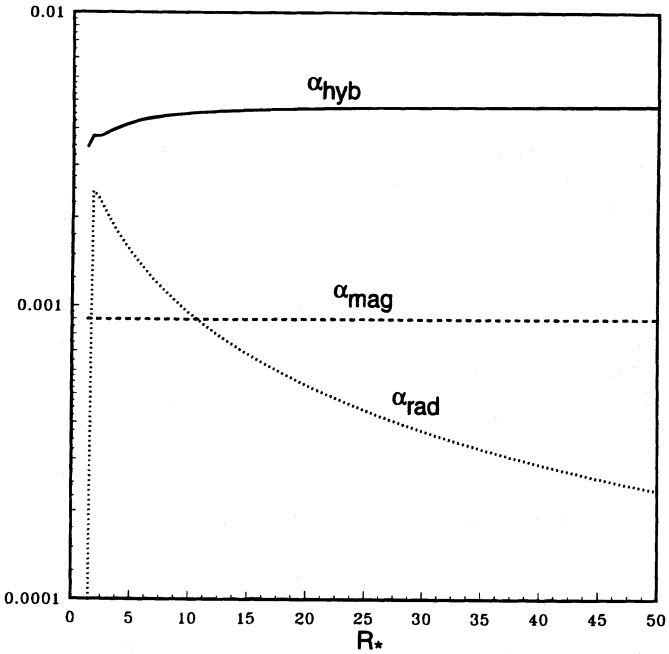

FIG. 2.—Results for α_{hyb}, α_{mag}, and α_{rad} for model a (see Fig. 1), with $\dot{M}/\dot{M}_E = 0.0025$ and $\xi = 0.03$.

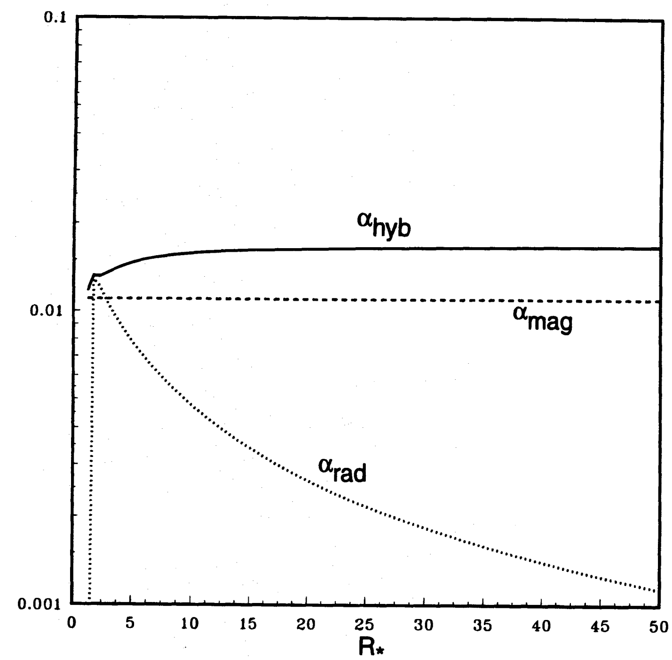

FIG. 4.—Results for α_{hyb}, α_{mag}, and α_{rad} for model b (see Fig. 1), with $\dot{M}/\dot{M}_E = 0.0375$ and $\xi = 0.105$.

value of $\xi \equiv \lambda_{coh}/H$ throughout the extent of the disk, which we take to be $R_{ms} < R_* < 50$, where R_{ms} is the radius of marginal stability in gravitational radii. It turns out that the condition $T_i/T_e > 1$ is satisfied for models for the entire parameter space shown in Figure 1. Models with parameters lying to the left of the dotted line are guaranteed to satisfy $H/R < 1$ for all radii. It follows that such models satisfy self-consistency constraints (i)–(iv) of § 3.2. Models with parameters lying below the solid line satisfy $\alpha_{hyb} > \alpha_{mag}$ for all radii, while those with parameters lying above the dashed line satisfy $\alpha_{hyb} > \alpha_{rad}$. The shaded region, therefore, is the one in which our models will be fully self-consistent. It may be emphasized that our calculations take only α_{hyb} into account; α_{mag} and α_{rad} are calculated a posteriori. Figure 1 therefore suggests the following:

(a) For sufficiently small $\xi \equiv \lambda_{coh}/H$ (approximately ≤ 0.1) hybrid viscosity dominates over magnetic viscosity.

(b) For sufficiently large accretion rates, the disk becomes puffy ($H/R > 1$) and the luminosity becomes high enough so that radiation viscosity dominates over hybrid viscosity. However, our models turn out to be optically thin to electron scattering in general. This means that the mean

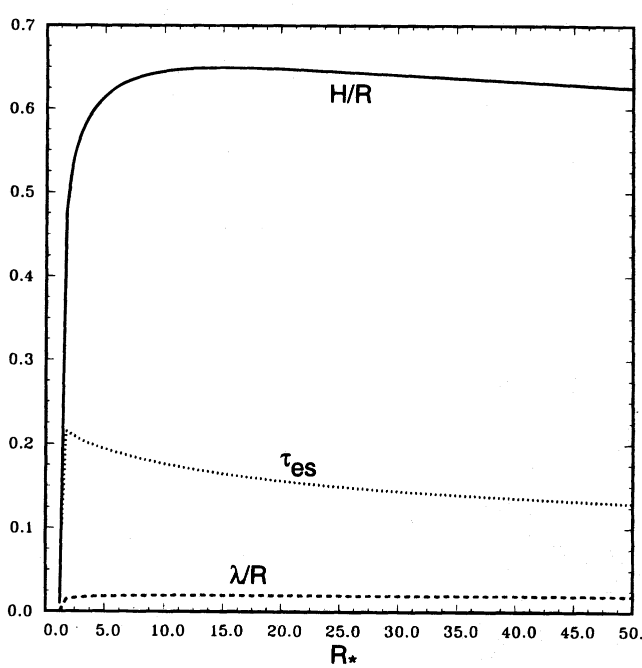

FIG. 3.—Results for H/R, λ/R, and τ_{es} for model a (see Fig. 1), with $\dot{M}/\dot{M}_E = 0.0025$ and $\xi = 0.03$.

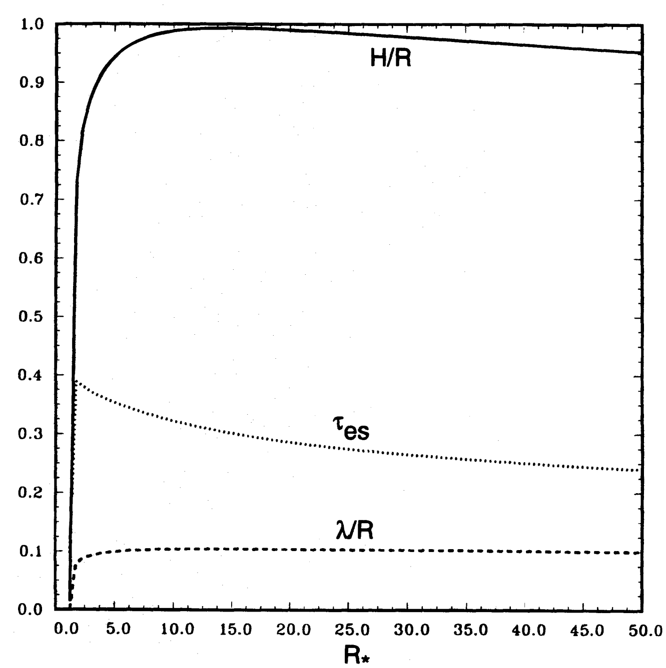

FIG. 5.—Results for H/R, λ/R, and τ_{es} for model b (see Fig. 1), with $\dot{M}/\dot{M}_E = 0.0375$ and $\xi = 0.105$.

free path for photons in the vertical direction is greater than the height H, and the radiation viscosity we calculate is therefore an *overestimate* of the actual value. It may also be noted that the breakdown of the thin disk condition implies a breakdown of the entire quasi-Keplerian structure and the radial velocity can no longer be ignored in comparison with the azimuthal velocity.

These statements, however, can only be taken to be indicative of general trends. It would require a self-consistent inclusion of all the different forms of viscosity in order to obtain more concrete conclusions in this regard. We are concerned only with demonstrating the applicability of the hybrid viscosity mechanism to accretion disks in this paper.

We next examine two specific models from the parameter space shown in Figure 1, models a and b. They serve as illustrations of a two-temperature accretion disk model that employs hybrid viscosity. Figures 2 and 3 show some physical quantities associated with model a, with $\dot{M}/\dot{M}_E = 0.0025$ and $\xi = 0.03$. Figure 2 shows that α_{hyb} is around 0.0045 and is also well in excess of α_{rad} and α_{mag}. Figure 3 shows that the disk is indeed thin and that $\lambda/R \ll 1$. Figures 4 and 5 show quantities associated with model b, with $\dot{M}/\dot{M}_E = 0.0375$ and $\xi = 0.105$. Figure 4 shows that α_{hyb} is around 0.017, and it is well in excess of α_{mag}. It exceeds α_{rad} in all but the innermost regions. Figures 3 and 5 also show that both the models are optically thin to electron scattering. We have verified that the radiation and magnetic pressures are much smaller than the gas pressure for both these models, thus justifying the assumption of gas pressure dominance. The ion temperatures for both these models are around 10^{12} K, while the electron temperatures are around 10^9 K.

4. DISCUSSION

We have derived a hybrid viscosity arising from momentum deposition by ions in the presence of a tangled magnetic field. This viscosity is neither the usual Coulomb viscosity which arises from Coulomb collisions between ions, nor is it pure magnetic viscosity, which is due to magnetic stresses. The tangled magnetic field plays a role in confining the ions, which makes the viscosity mechanism a local process. The field also acts as an intermediary in the momentum transfer between ions, in situations where the coherence length of the field $\lambda_{coh} \ll \lambda_{ii}$, where λ_{ii} is the usual Coulomb ion-ion mean free path. Upon application of this form of viscosity to a specific disk model, we observe that the self-consistency requirements limit valid models to sub-Eddington accretion rates. We also observe that the hybrid viscosity dominates over magnetic viscosity for small values of ξ. The only restriction on the magnitude of the magnetic field in our calculations is that it be at least so large as to warrant the assumption of nearly zero gyroradii for the ions.

We have entirely neglected any momentum transfer arising out of short-wavelength plasma waves in the accretion flow. Since the tangled magnetic field is taken to be arising from plasma turbulence, the presence of such waves is quite plausible, and it is one aspect of the problem we have neglected in our calculations. In fact, ion streaming along magnetic field lines, which is considered to be the primary means of momentum transfer in this paper, might very well be the source of such waves if their speeds are super-Alfvénic. One could model an ensemble of such turbulent plasma waves as a collection of plasmons, assign a number density and mass to these entities, and investigate their role as intermediaries in momentum transfer. A self-consistent calculation of the tangled magnetic fields arising as a consequence of the presence of plasma turbulence could also reveal magnetic flutter; temporal variations in the local magnetic field (as distinct from the large-scale evolution of the fields due to dynamo action) that we have also neglected.

In the present work we have adopted a time-independent treatment. There have been a number of investigations of possible disk instabilities (Shakura & Sunyaev 1976; Piran 1978, for instance) which consider the presence of thermal and viscous instabilities that could break up the disk and cause variations in the disk luminosity. The temperature-dependent nature of any viscosity in which ions play a part (like the hybrid viscosity discussed in this paper) would result in a coupling of viscous and thermal instabilities. We are currently in the process of undertaking an investigation of these aspects. It may also be noted that advection effects can assume importance and alter the disk structure near the inner edge.

We would like to thank Dr. Ethan Vishniac and the anonymous referee for several useful criticisms and suggestions. P.S. also acknowledges useful discussions with Dr. Ulf Torkelsson.

APPENDIX A

CONSTITUTIVE EQUATIONS FOR TWO-TEMPERATURE, COMPTONIZED MODEL

The basic disk structure equations are the same as those used in the disk structure calculations of Eilek & Kafatos (1983), which neglect radiation pressure:

$$P = \frac{GMm_i N_i H^2 f_1}{R^3}, \tag{A1}$$

$$\alpha P = \frac{(GMR)^{1/2}\dot{M} f_2}{4\pi R^2 H}, \tag{A2}$$

$$\frac{3}{8\pi}\frac{GM\dot{M}}{R^3 H} f_3 = 3.75 \times 10^{21} m_i \ln\Lambda N_i^2 k \frac{(T_i - T_e)}{T_e^{3/2}}, \tag{A3}$$

$$P = N_i k(T_i + T_e) , \tag{A4}$$

$$T_e = \frac{m_e c^2 y}{4k} \frac{1}{\tau_{es} g(\tau_{es})} , \tag{A5}$$

$$\tau_{es} = N_i \sigma_T H , \tag{A6}$$

where σ_T is the Thomson scattering cross section. The Coulomb logarithm $\ln \Lambda$ is taken to be 15 in our numerical calculations and the function $g(\tau_{es}) \equiv 1 + \tau_{es}$. It may be noted that this is different from the form for $g(\tau_{es})$ used by Eilek & Kafatos (1983). The factors f_1, f_2 and f_3 are the relativistic correction factors appropriate to the metric under consideration. These factors for a Kerr black hole with $a/M = 0.998$ are used in Eilek & Kafatos (1983). Eilek (1980) gives plots of f_1, f_2, and f_3 for a Kerr black hole. The relativistic correction factors appropriate to a Schwarzschild metric can be obtained by setting $a/M = 0$ in the expressions for f_1, f_2, and f_3. In keeping with the convention used in Eilek & Kafatos (1983), we make the definitions $M_8 \equiv M/10^8\ M_\odot$, $\dot{M}_* \equiv \dot{M}/1\ M_\odot\ \text{yr}^{-1}$, and $R_* \equiv R/(GM/c^2)$. If we assume $T_i \gg T_e$, equations (A1)–(A6) yield the following analytical solutions:

$$T_i = 4.99 \times 10^{13} \frac{\dot{M}_*}{M_8} f_2 \tau_{es}^{-1} \alpha^{-1} R_*^{-3/2} , \tag{A7}$$

$$T_e = 1.40 \times 10^9 y \tau_{es}^{-1} [g(\tau_{es})]^{-1} , \tag{A8}$$

$$N_i = 4.70 \times 10^{10} \left(\frac{\dot{M}_*}{M_8}\right)^{1/2} \dot{M}_*^{-1} f_1^{1/2} f_2^{-1/2} \tau_{es}^{3/2} \alpha^{1/2} R_*^{-3/4} . \tag{A9}$$

It may be emphasized that α is a free parameter in the above solutions.

APPENDIX B

DEFINITION OF RADIATION VISCOSITY

We use α_{rad}, the α parameter obtained from radiation viscosity, as a diagnostic in this paper. We now proceed to define the manner in which we compute α_{rad}. We follow Shapiro et al. (1976) in defining the radiation energy density using

$$U_{rad} = (F/c) g(\tau_{es}) . \tag{B1}$$

If the y parameter is taken to be equal to unity, eliminating $g(\tau_{es})$ between equations (A5) and (B1), using equation (A6) yields

$$\frac{F}{H} = \left(\frac{4kT_e}{m_e c^2}\right) N_i \sigma_T c U_{rad} , \tag{B2}$$

where F is the dissipated energy density. Equation (A3) is another way of defining F/H; in fact, F has to be equal to $(3/8\pi) GM\dot{M}/R^3$ for the disk to be quasi-Keplerian. Equating the right-hand side of equation (A3) to that of equation (A8) and assuming $T_i \gg T_e$ yields

$$U_{rad} = 9.565 \times 10^5 N_i T_i T_e^{-5/2} . \tag{B3}$$

We next adopt the definition of radiation viscosity η_{rad} given by Loeb & Laor (1992),

$$\eta_{rad} = \frac{8}{27} \frac{U_{rad}}{N_i \sigma_T c} . \tag{B4}$$

We calculate α_{rad} by adopting the usual definition for α, akin to equation (3.4),

$$\alpha_{rad} P \equiv -R \eta_{rad} \frac{d\Omega_{kepl}}{dR} . \tag{B5}$$

It may be noted that we assume the disk to be gas-pressure dominated; although we do calculate α_{rad} as a diagnostic tool, P in equation (B4), which represents total pressure, does not include radiation pressure in our calculations.

This yields

$$\frac{\alpha_{rad}}{\alpha_{hyb}} = \frac{\eta_{rad}}{\eta_{hyb}} = 6.45 \times 10^{33} \delta^{-1} \ln \Lambda T_i^{-3/2} T_e^{-5/2} , \tag{B6}$$

where δ is defined in equation (3.10).

REFERENCES

Begelman, M. C., & Chiueh, T. 1988, ApJ, 332, 872

Brandenburg, A., Nordlund, A., Stein, R. F., & Torkelsson, U. 1995, ApJ, 446, 741

Eardley, D. M., & Lightman, A. P. 1975, ApJ, 200, 187

Eilek, J. A. 1980, ApJ, 236, 644

Eilek, J. A., & Kafatos, M. 1983, ApJ, 271, 804

Filho, C. M. 1995, A&A, 294, 295

Goldman, I., & Wandel, A. 1995, ApJ, 443, 187

Hawley, J. F., Gammie, C. F., & Balbus, S. A. 1995, ApJ, 440, 742

Kafatos, M. 1988, in Supermassive Black Holes (Cambridge: Cambridge Univ. Press), 307

Katz, J. I. 1991, ApJ, 367, 407

Kaufman, A. 1960, La Theorie dez Gas Neutres et Ionizes (Paris: Hermann et Cie)
Loeb, A., & Laor, A. 1992, ApJ, 384, 115
Matsumoto, R., & Tajima, T. 1995, ApJ, 445, 767
Mihalas, D., & Mihalas, B. W. 1984, Foundations of Radiation Hydrodynamics (New York: Oxford Univ. Press)
Paczyński, B. 1978, Acta Astron., 28, 253
Piran, T. 1978, ApJ, 221, 652
Pringle, J. E. 1981, ARA&A, 19, 137
Schramkowski, G. P., & Torkelsson, U. 1996, A&AR, in press
Shapiro, S. L., Lightman, A. L., & Eardley, D. M. 1976, ApJ, 204, 187
Shakura, N. I., & Sunyaev, R. A. 1973, A&A, 24, 337
———. 1976, MNRAS, 175, 613
Spitzer, L. 1962, Physics of Fully Ionized Gases (New York: Interscience)